Malaysian Journal of Catalysis

MJCat

Research Article

Characterisation of Fe-doped mesoporous silica nanoparticles for CO₂ methanation

M.A.A. Aziz[a,*], A.A. Jalil[a,b], S. Triwahyono[c]

[a]*Department of Chemical Engineering, Faculty of Chemical and Energy Engineering, Universiti Teknologi Malaysia, 81310 UTM Johor Bahru, Johor, Malaysia*
[b]*Centre of Hydrogen Energy, Institute of Future Energy, Universiti Teknologi Malaysia, 81310 UTM Johor Bahru, Johor, Malaysia*
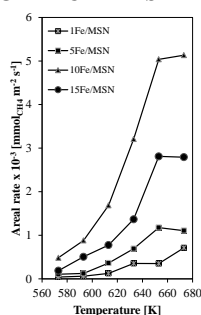[c]*Department of Chemistry, Faculty of Science, Universiti Teknologi Malaysia, 81310 UTM Johor Bahru, Johor, Malaysia.*
Corresponding author email: arif@cheme.utm.my

GRAPICAL ABSTRACT

ABSTRACT

Fe metal catalysts supported on mesoporous silica nanoparticles (MSN) with various Fe loadings (1-15 wt%) have been prepared by the incipient wetness impregnation method. The results obtained revealed that increasing Fe loading (1–15 wt.%) decreased the crystallinity of MSN and N_2 adsorption as evidenced by XRD and N_2 physisorption, respectively. ^{29}Si NMR results showed that increasing Fe loading affected the arrangement of the Si atom by increasing the population of Q2 with a concomitant decrease of Q3 and Q4. The addition of Fe on MSN also increased the mononuclear cations, oligomeric and bulky Fe oxide (Fe_2O_3) species in MSN. The catalyst activities on CO_2 methanation followed the order 10Fe/MSN > 15Fe/MSN > 5Fe/MSN > 1Fe/MSN. The high activity of 10Fe/MSN may be related to its structural properties tailored by all Fe species on the MSN surface. Based on these results, it may be concluded that the CO2 methanation over Fe/MSN catalysts depends on the Fe oxide species, catalysts structure of particle size and pore volume, and an appropriate amount of Fe species on the surface of MSN.

Key words: CO_2 methanation, mesoporous silica nanoparticles, Fe catalyst

1. INTRODUCTION

The increased awareness of the environmental impact of CO_2 has led to several R&D efforts to bind CO_2 over the last few years. Proposals have ranged from capturing CO_2 either directly from the flue gas emitted by heavy industries or from the atmosphere by binding it in inorganic oxides [1]. Once captured, CO_2 is either sequestered or catalytically converted to more valuable products. In this case, CO_2 methanation could be a method for the conversion of CO_2 with H_2 to CH_4. This process has recently regained interest for the selective production of value-added products not only from CO but also from the greenhouse gas CO_2 [2].

CO₂ hydrogenation to methane has been widely explored in recent years [3-4]. The catalysts employed are mainly concentrated on Ni-based catalysts. However, Ni-based catalysts are not selective and are subject to coking [5], which lowers the efficiency of methanation. Catalytic selectivity and stability of metal catalysts are affected by many factors such as metal loading, promoters, supports, catalyst preparation procedure, and experimental conditions. The metal loading on the support affected both the interaction of metal with the support and the metal dispersion on the support (metal particle sizes), which further affected the catalytic behaviours during methanation. In general, the metal species tended to be highly dispersed across the carrier at low metal loadings, whereas the metal particles tended to aggregate at high metal loadings, forming large particles [6]. Understanding this relationship can help researchers understand dispersion–activity relationships and prepare active, selective, and stable metal catalysts. Fe embedded on mesoporous silica catalysts have been identified as an important material and have been widely used in many fields including healthcare [7], optics [8], catalysis [9], and environmental remediation [10]. Discrete nanoparticles with core–shell structures are of a particular interest due to their high surface areas, improved suspendibility, faster mass transport, and large amount of accessible pore volume [11]. In addition, newly potential mesoporous silica nanoparticles (MSN) can provide attractive and effective ways to enhance the activity of catalytic reactions [3]. This is due to their distinctive properties such as nanosize, ordered porous structure, unique pores type (intra and interporosity), extremely high surface area (>1000 m²/g), large pore volume, and well-defined and tunable pore size (1.5–10 nm). The pore diameters also can be tailored to host specific particles according to their dimensions [12]. These properties are necessary in sorption and catalysis applications, while maintaining the intrinsic properties of silica.

In the present study, the synergy of Fe catalyst and MSN was tested on CO_2 methanation. To this date, the detailed study of Fe promoted on MSN for CO_2 methanation has not been reported yet. Therefore, this present paper focuses on the effects of Fe doped on MSN on the performance of CO_2 methanation. This study also varied the Fe loading as to determine the suitable amount of Fe on MSN for high activity of the reaction. Characterization data is discussed using X-ray diffraction (XRD), N_2 adsorption–desorption, ^{29}Si NMR, and UV- visible diffuse reflectance (UV-Vis-DR) spectroscopy.

2. EXPERIMENTAL

2.1 Catalyst preparation

MSN was prepared by the sol–gel method according to the previous report [13]. The surfactant cetyltrimethylammonium bromide (CTAB; Merck), ethylene glycol (EG; Merck), and NH₄OH solution (QRec) were dissolved in water with the following molar composition of CTAB : EG :

$NH_4OH : H_2O = 0.0032 : 0.2 : 0.2 : 0.1$. After vigorous stirring for about 30 min at 353 K, 1.2 mmol of tetraethyl orthosilicate (TEOS; Merck) and 1 mmol of 3-aminopropyl triethoxysilane (APTES; Merck) were added to the clear mixture to give a white suspension solution which eventually became gel-like. This solution was then stirred for another 2 h, and the samples were collected by centrifugation at 20,000 rpm. The synthesized MSN was dried at 333 K and calcined at 823 K for 3 h in air to remove the surfactant. Fe doped MSN catalysts were prepared by impregnation of MSN powder with an aqueous solution of Fe salt precursor, $Fe(NO_3)_3$ (Merck, 99%). The resulting slurry was heated slowly at 353 K under continuous stirring and maintained at that temperature until nearly all the water was evaporated. The solid residue was dried in an oven at 383 K overnight before calcination at 823 K for 3 h in air. The Fe loadings of the catalysts thus prepared were 1, 5, 10, and 15 wt.%, and were denoted as 1Fe/MSN, 5Fe/MSN, 10Fe/MSN, and 15Fe/MSN, respectively.

2.2 Characterization

The crystalline structure of the catalyst was determined with X-ray diffraction (XRD) recorded on a powder diffractometer (Bruker Advance D8, 40 kV, 40 mA) using a Cu Kα radiation source in the range of $2\theta = 1.5–90°$. The BET analysis of the catalyst was determined by N_2 adsorption–desorption isotherms using a Quantachrome Autosorb-1 instrument. The catalyst was outgassed at 573 K for 3 h before being subjected to N_2 adsorption. Pore size distributions and pore volumes were determined from the sorption isotherms using a non-localized density functional theory (NLDFT) method. Nuclear magnetic resonance measurements were carried out using ^{29}Si magic angle spinning nuclear magnetic resonance (MAS-NMR) Spectroscopy, which was performed at room temperature on a Bruker Solid NMR (JEOL 400 MHz) spectrometer using tetramethylsilane (TMS) as an external reference. The spectra were recorded using 4 μs radio frequency pulses, a recycle delay of 60 s and spinning rate of 7 kHz using a 4 mm zirconia sample rotor. UV–vis diffuse reflectance spectroscopy (UV–vis–DRS) measurements were performed on fine powders of the Fe-samples put into a cell with optical quartz walls by a Perkin Elmer Ultraviolet-visible Spectrometer Lambda 900 in the range of 200–800 nm.

2.3 Catalytic testing

CO_2 methanation was conducted in a fixed-bed quartz reactor with an interior diameter of 8 mm at atmospheric pressure at a temperature range of 573-673 K. The thermocouple was directly inserted into the catalyst bed to measure the actual pretreatment and reaction temperatures. The catalyst was sieved and selected in the 20-40 μm fraction. Initially, 200 mg of catalyst were treated in an oxygen stream ($F_{Oxygen} = 100$ ml/min) for 1 h followed by a hydrogen stream ($F_{Hydrogen} = 100$ ml/min) for 4 h at 773 K and cooled down to the desired reaction temperature in a hydrogen stream. After the temperature became stable, a mixture of H_2 and CO_2 was fed into the reactor at a specific gas hourly space velocity (GHSV) and H_2/CO_2 mass ratio. All gases were controlled with calibrated mass flow controllers (SEC-400 MK2, Stec Ltd., Japan). The

activity was monitored by decreasing and raising the temperature to verify the stable catalyst conditions during these measurements. The composition of the outlet gases was analysed with an on-line 6090N Agilent gas chromatograph equipped with a GS-Carbon PLOT column and a TCD detector. The lines from the outlet of the reactor to the GC were heated at 383 K to avoid condensation of the products. The moisture trap was installed at the outlet gas line of the reactor to prevent moisture from entering the GC. To determine the activity, the products were collected after 1 h of steady-state operation at each temperature. The conversion of carbon dioxide, selectivity of products, and areal rate of methane formation were calculated by the following equations:

$$X_{CO2}(\%) = \frac{F_{CO2,in} - F_{CO2,out}}{F_{CO2,in}} \times 100\% \qquad (1)$$

$$S_x(\%) = \frac{F_{x,out}}{F_{CO2,in} - F_{CO2,out}} \times 100\% \qquad (2)$$

$$Areal\ rate\ (mmol_{CH4} \cdot m^{-2}s^{-1}) = \frac{F_{x,out}}{S_{BET} \times W_{cat}} \qquad (3)$$

where X_{CO2} is the conversion of carbon dioxide (%), S_x is the selectivity of x product (%) in which x is a CH_4 or CO, F is a molar flow rate of CO_2 or product in mole per second, S_{BET} is the surface area of the catalysts, and W_{cat} is the weight of catalysts.

3. RESULTS AND DISCUSSION

FESEM image of 10Fe/MSN sample showed nano-sized catalysts with particle sizes of approximately 100 nm (Fig. 1A). The catalyst was then characterized by XRD to ascertain the formation of new active phase structures in the solid catalyst, which is believed to have been responsible for its performance during the activity testing. Fig. 1B shows the low-angle XRD patterns of MSN and Fe-based MSN catalysts. The patterns exhibit three main peaks at 2.25°, 3.8°, and 4.4° which were indexed as (100), (110), and (200), respectively. These peaks are reflections of typical two dimensional, hexagonally ordered mesostructures (p6mm), demonstrating the high quality of the mesopore packing. The XRD pattern of Fe/MSN revealed that the Fe metal presence during the silica gel synthesis strongly affected the hexagonal symmetry of silica, as can be verified by the decrease in the relative intensity of the d_{100} reflection as compared to the same peak in the MSN.

On the other hand, Fe/MSN has experienced a structural degradation of MSN albeit no shift in the peaks at 2.25°, 3.8°, and 4.4° were observed. The presence of Fe oxide crystallites phase on the catalysts were characterized using wide-angle XRD (10°-90°), as shown in Fig. 1C, in which the diffraction peaks at 24.1°, 33.2°, 35.5°, 40.8°, 49.4°, 53.9°, 62.6°, and 64.1° were indexed to the rhombohedral crystalline structure of α-Fe_2O_3 (JCPDS: 01-089-8103). No α-Fe_2O_3 crystalline phase was observed on 1Fe/MSN. Two peaks at 33.2° and 35.5° of α-Fe_2O_3 phase were observed on 5Fe/MSN. Three peaks were observed at 33.2°, 35.5°, and 53.9° on 10Fe/MSN and 15Fe/MSN which may indicate a strong bond between the Fe and MSN support. The low XRD intensity of Fe crystalline on MSN support may be due to the low amount of Fe content loading on MSN support and higher dispersion.
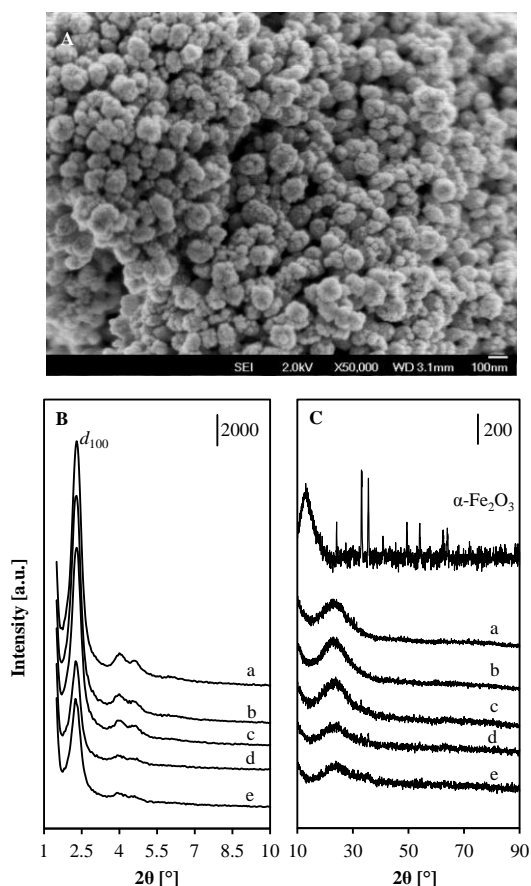
Fig. 1 (A) FESEM image of 10Fe/MSN. Low angle (B) and wide angle (C) XRD patterns of (a) MSN, (b) 1Fe/MSN, (c) 5Fe/MSN, (d) 10Fe/MSN, and (e) 15Fe/MSN.

The porosity of the catalysts was measured by the N_2 physisorption method. It is well known that the location of the inflection point is related to a pore in the mesoscale and that the sharpness of these curves reveals the uniformity of the mesopore size distribution [14]. Fig. 2A and B show the adsorption–desorption isotherms and pore size distribution, respectively, for all catalysts. All isotherm curves exhibited two capillary condensation steps. The first step, in a relative pressure range of P/Po = 0.3–0.4, was attributed to the nitrogen condensation that took place in the internal mesopores.
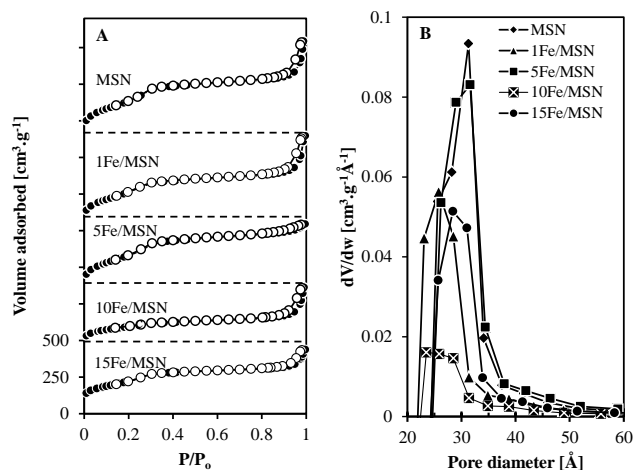
There was no hysteresis loop in this capillary condensation. The second step, above P/Po = 0.95 in the adsorption branch, was due to the presence of interparticle voids. A small hysteresis loop at this relative pressure was ascribed to the condensation of nitrogen within the interstitial voids or to the interparticle textural porosity created by MSN particles, which indirectly reflects the size of particles, that is, a higher partial pressure was associated with a smaller particle size. However, upon increasing the Fe loading from 1 to 15 wt.%, both capillary condensation steps decreased simultaneously. For 10Fe/MSN, the first step almost disappeared, whereas the second step decreased by almost 40%. The increment on the second step of 10Fe/MSN may indicate that the sizes of MSN particle were smaller compared to 5Fe/MSN and 15Fe/MSN. Meanwhile, as shown in Figure 2B, by comparing the pore size distribution of different samples, a declining trend of pore size is detected with the increase of the loading of Fe species. Noticeably, the numbers of micropores increase accordingly due to the gradual introduction of Fe species. Herein, the generation of micropore is attributed to the occupation of Fe species in the mesochannel of silica. As a result, the pore volumes of MSN were gradually increased by increasing the number of Fe species from 1 wt.% to 10 wt.% Fe loading on the MSN except for 15 wt.% Fe loading on MSN which shows a slight decrease in pore size, corresponding to pore blockage. In addition, with the growing amount of Fe species incorporated in channels, it is notable that the surface areas of all the samples decreased. These results demonstrate the presence of Fe species in the channels of mesoporous silica. In addition, the wall thickness expands after the introduction of Fe species, which could be attributed to the Fe oxide layer presenting in the pore wall.

Table 1. Physicochemical properties of calcined MSN and Fe/MSNs catalysts

Catalyst	S_{BET}^a $(m^2 \cdot g^{-1})$	V_{Total}^a $(cm^3 \cdot g^{-1})$	d_{avg}^a (Å)	Relative crystallinity[b] (%)
MSN	1025	0.725	28	100
1Fe/MSN	973	0.752	31	91
5Fe/MSN	1046	0.846	32	79
10Fe/MSN	487	0.444	36	42
15Fe/MSN	627	0.502	32	40

[a] Specific surface area, pore volume and average pore diameter were calculated using the BET method.
[b] Relative crystallinity determined by XRD.

However, the results of the BET surface area, total pore volume, and average pore diameter showed inconsistencies upon Fe loading which may have been affected during catalysts preparations such as temperature effect, stirring effect, and mixing effect (Table 1). For instance, the BET surface area of 5Fe/MSN was shown to be higher than MSN. This may be due to the contribution of pores generated from the Fe species agglomerated on the surface of the catalyst during the catalyst preparation as evidenced from the higher total pore volume of the catalyst. High average pore diameter of 10Fe/MSN may indicate the Fe species were dispersed mainly on the outer surface of MSN support; while, the lower pore volume of 10Fe/MSN may be attributed to the pore blockage of Fe species.

The ^{29}Si NMR spectra of MSN and Fe/MSN depicted in Fig. 3, shows three different signals at −92, −102, and −110 ppm, similar to that obtained for doped mesoporous silica as

Fig. 2 (A) N_2 adsorption–desorption isotherm and (B) pore size distribution of all catalysts.

reported in literature [15]. There are marked differences in the Si distribution between these samples. To illustrate the presence of different Si environments, the NMR spectra were converted into three simulated peaks by fitting the curves with a Gaussian function. These three peaks at -92, -102, and -110 ppm were assigned to Si atoms with two (Q2), three (Q3), and four (Q4) siloxy bonds, respectively. The ratios of the various types of Si are also presented in the figure. For MSN, the percentage of intensities of three Si peaks (Q2:Q3:Q4) are 14:34:52. These values changed to 14:33:53 and 14:32:54 in 1Fe/MSN and 5Fe/MSN, respectively, showing a decrease in Q3 and increase in Q4. The population of the Q3 and Q4 environment slightly decreased after the introduction of 15 wt.% Fe loading on MSN. The percentage of intensities of three Si peaks was changed to 15:32:53 and 32:28:40 in 10Fe/MSN and 15Fe/MSN, respectively. The result of 10Fe/MSN and 15Fe/MSN showed slightly constant Q3 values while there was a marked increase in Q2 and decrease in Q4 values. A marked decrease in the intensity of the Q3 signal in comparison with metal-free MSN is observed, which verified the tethering of the functional groups to Si–OH. The result also confirm that most of the Fe species are not in the silica network. This kind of trend is also reported in literature [16].
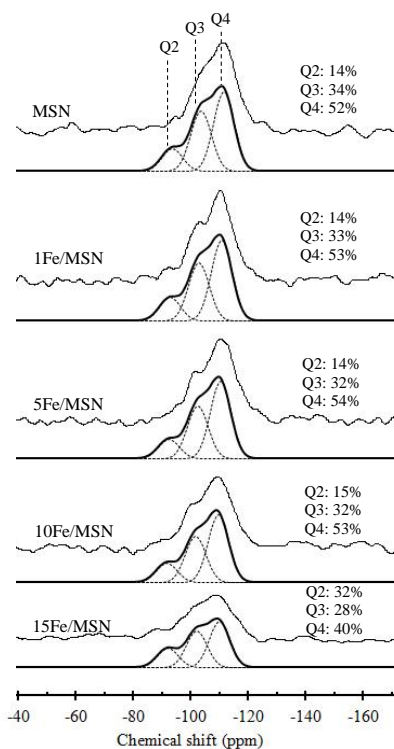

Fig. 3 ^{29}Si NMR spectra of MSN and Fe/MSNs

The chemical nature of transition metals species deposited on the surface of MSN was studied by UV–vis-DR spectroscopy. The results of these studies for the Fe/MSNs are shown in Fig. 4. It should be mentioned that the presented spectra are the results of the subtraction of the original spectra recorded for the MSN from the original spectra of Fe/MSNs, thus demonstrating that it is related only to the state of the metal. The spectra recorded for the Fe/MSNs were fitted with three bands centred at about 260 nm, 360 nm, and 516 nm. The first band is related to the presence of mononuclear Fe^{3+}

ions in the octahedral coordination while the second one corresponds to small oligonuclear $(FeO)_n$ clusters [17]. The band at 516 nm was attributed to the presence of bulky Fe oxide (Fe_2O_3) clusters [18]. The results showed that the contribution of the oligomeric and bulky Fe oxide (Fe_2O_3) species significantly increased when the Fe loading on MSN was higher than 5 wt.% , while a significant contribution of Fe in the form of mononuclear cations were found only on 1Fe/MSN. Therefore, it seems that Fe deposited on the surface of MSN for more than 5 wt.% Fe loading is present exclusively in the form of mononuclear cations, oligomeric, and bulky Fe oxide (Fe_2O_3) metal oxide clusters which are more catalytically active than those in the form of mononuclear Fe species only.
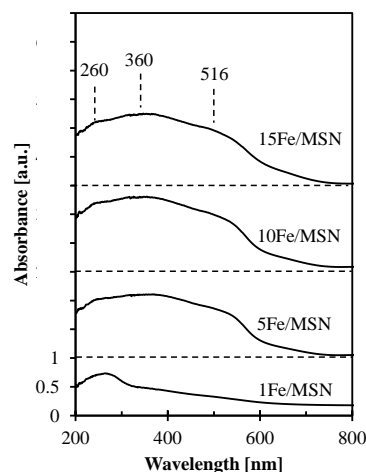

Fig. 4 Differential UV–vis-DR spectra of the Fe/MSNs

The effect of Fe loading on CO_2 methanation over Fe/MSN was investigated and the results are depicted in Fig. 5, where the yield of methane formation is plotted as a function of reaction temperature in the range of 573-673 K. No methane formation was observed for bare MSN catalyst which was due to the absence of metal sites, which is crucial for H_2 and CO_2 dissociation. S-curve results were observed for all Fe/MSN catalysts, indicating that the production rate for methane was not influenced by intraparticle diffusion of the catalysts under the reaction conditions. Furthermore, it was observed that the order of activity for CO_2 methanation at 673 K was 10Fe/MSN > 15Fe/MSN > 5Fe/MSN > 1Fe/MSN. All catalysts that began the reaction at 573 K and 10Fe/MSN exhibited a better result at all ranges of temperatures compared to others. Regarding the product selectivity, the major products were always methane; no C_2 or heavier hydrocarbons were observed in this experiment. This higher activity of 10Fe/MSN can be related to an appropriate amount of Fe species on the outer surface of MSN support which is due to the filling of Fe species in the pore volume of MSN. Therefore, CO_2 and H_2 molecules may have easily passed through and actively reacted at the outer surface of the catalyst.

As was shown by ^{29}Si NMR and UV–vis–DR spectra studies, Fe was present mainly on the outer surface of the MSN and in the form of mononuclear Fe^{3+} ions, small oligonuclear $(FeO)_n$ clusters, and bulky Fe oxide clusters species. The presence of three species of mononuclear cations, oligomeric, and bulky Fe oxides on MSN may be responsible for

their high catalytic activity in the CO_2 methanation in comparison to only mononuclear Fe^{3+} species on MSN (i.e 1Fe/MSN). Smaller catalyst particles may have also contributed to the high activity of 10Fe/MSN compared to 1Fe/MSN and 5Fe/MSN, as evidenced from the capillary condensation steps in Nitrogen isotherm. Lower pore volume of 10Fe/MSN may also indicate that the catalytic activity may actively occur on the surface of the catalyst. Based on these results, it may be concluded that the catalytic activity depends on the Fe oxide species, catalysts structure of particle size, pore volume, and an appropriate amount of Fe species on the surface of MSN.
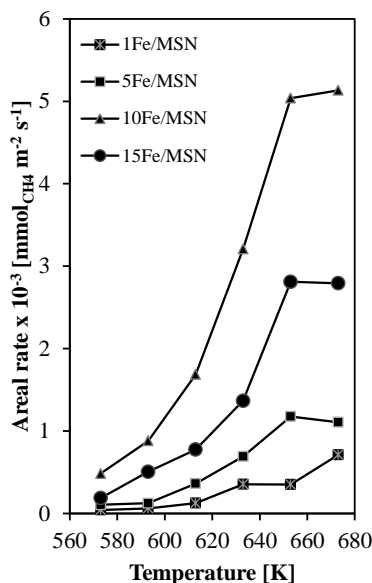

Fig. 5 Effect of reaction temperature on methane formation in CO_2 methanation

4.   CONCLUSION

Mesoporous silica nanoparticles were modified using 1-15 wt,% of Fe with the wet impregnation method. XRD, N_2 physisorption, FESEM, ^{29}Si NMR, and UV-visible diffuse reflectance (UV-Vis-DR) spectroscopy analyses were used to characterise the catalysts. From the results, it was found that the high activity of Fe/MSN with 10 wt.% Fe loading toward the methanation of CO_2 is related to its structural properties tailored by bulky Fe species on the MSN surface. The increasing Fe loading (1-15 wt%) also affected the arrangement of Si atoms by increasing the population of Q2 with a concomitant decrease of Q3 and Q4. The presence of three species of mononuclear cations, oligomeric, and bulky Fe oxide on MSN may be responsible for their high catalytic activity in the CO_2 methanation in comparison to only mononuclear Fe^{3+} species on MSN (i.e 1Fe/MSN). Smaller catalyst particles may have also contributed to the high activity of 10Fe/MSN compared to 1Fe/MSN and 5Fe/MSN as evidenced from the capillary condensation steps in the nitrogen isotherm. Based on these results, it may be concluded that the CO2 methanation over Fe/MSN catalysts depends on the Fe oxide species, catalysts structure of particle size, pore volume, and an appropriate amount of Fe species on the surface of MSN.

REFERENCES

[1]   J. Gao, Q. Liu, F. Gu, B. Liu, Z. Zhong and F. Su, RSC Adv. 5 (2015) 22759.
[2]   D. Cui, J. Liu, J. Yu, J. Yue, F. Su and G. Xu, RSC Adv. 5 (2015) 10187.
[3]   M. A. A. Aziz, A. A. Jalil, S. Triwahyono and S.M. Sidik, Appl. Catal. A. 486 (2014) 115.
[4]   L. P. Teh, S. Triwahyono, A. A. Jalil, R. R. Mukti, M. A. A. Aziz and T. Shishido, Chem. Eng. J. 270 (2015) 196.
[5]   J. Gao, C. Jia, J. Li, F. Gu, G. Xu, Z. Zhong, F. Su, *Ind. Eng. Chem. Res.* 51 (2012) 10345.
[6]   S. M. Sidik, S. Triwahyono, A. A. Jalil, M. A. A. Aziz, N. A. A. Fatah, L. P. Teh, J. CO₂ Util. 13 (2016) 71.
[7]   F. Yang, S. Gao, C. Xiong, S. Long, X. Li, T. Xi and Y. Kong, RSC Adv. 5 (2015) 72099.
[8]   K. R. Hurley, Y.-S. Lin, J. Zhang, S. M. Egger and C. L. Haynes, Chem. Mater. 25 (2013) 1968.
[9]   J. Wang, C. Liu, L. Tong, J. Li, R. Luo, J. Qi, Y. Li and L. Wang, RSC Adv. 5 (2015) 69593.
[10]   Y. Xie, W. Cheng, P. E. Tsang and Z. Fang, J. Environ. Manage. 166 (2016) 478.
[11]   N. Song and Y.-W. Yang, Chem. Soc. Rev. 44 (2015) 3474.
[12]   V. Hulea, D. Brunel, A. Galarneau, K. Philippot, B. Chaudret, P.J. Kooyman, F.Fajula, Microporous Mesoporous Mater. 79 (2005) 185.
[13]   M. A. A. Aziz, A. A. Jalil, S. Triwahyono, M. W. A. Saad, Chem. Eng. J. 260 (2015) 757.
[14]   J. H. de Boer, B. G. Linsen and T. J. Osinga, J. Catal. 4 (1965) 643.
[15]   S. Mandal, C. Santra, R. Kumar, M. Pramanik, S. Rahman, A. Bhaumik, S. Maity, D. Sen and B. Chowdhury, RSC Adv. 4 (2014) 845.
[16]   S. Xu, E. D. Walter, Z. Zhao, M. Y. Hu, X. Han, J. Z. Hu, X. Bao, J. Phys. Chem. C 119 (2015) 21219.
[17]   J. Pérez-Ramirez, M. S. Kumar and A. Brückner, J. Catal. 223 (2004) 13.
[18]   E. Suzuki, K. Nakashiro and Y. Ono, Chem. Lett. (1998) 953.